Electronic Supplementary Material (ESI) for Polymer Chemistry.
This journal is © The Royal Society of Chemistry 2021

Supplementary Information

for

Structure and Activity Relationship Studies of *N*-Heterocyclic Olefins and Thioureas/Ureas Catalytic System: Application in Ring-opening Polymerization of Lactones

Li Zhou ‡[a], Zhenyu Wang ‡[a], Guangqiang Xu *[a,b], Chengdong Lv [a,b], Qinggang Wang *[a,b]

[a] Key Laboratory of Biobased Materials, Qingdao Institute of Bioenergy and Bioprocess Technology, Chinese Academy of Sciences, Qingdao, 266101, China. E-mail: wangqg@qibebt.ac.cn.

[b] Center of Materials Science and Optoelectronics Engineering, University of Chinese Academy of Sciences, Beijing, 100049, China.

Table of Contents

1. General Experimental Procedure 3

Preparation of NHOs 3

Preparation of TUs/Us 3

2. pK_a determination of NHOs 4

Figure S1. ^{1}H NMR of NHOs and BnOH 5

Figure S2. ^{1}H NMR of NHO5 precursor salt, ^{t}Bu-P$_1$ and combinations 5

Figure S3. ^{1}H NMR of NHO5 precursor salt, ^{t}Bu-P$_2$ and combinations 6

Figure S4. ^{1}H NMR of NHO1 precursor salt, DBU and combinations 6

Figure S5. ^{1}H NMR of NHO1, TU5 and combinations 7

Figure S6. ^{1}H NMR of NHO2, TU5 and combinations 7

Figure S7. ^{1}H NMR of NHO3, U8 and combinations 8

Figure S8. ^{1}H NMR of NHO3 and U6 8

Figure S9. ^{1}H NMR of NHO3, U5 and combinations 9

Figure S10. ^{1}H NMR of NHO3 and U5 9

3. ^{1}H NMR Spectra 9

Figure S11. Homonuclear decoupled ^{1}H NMR 10

Figure S12. Homonuclear decoupled ^{1}H NMR 11

Figure S13. Homonuclear decoupled ^{1}H NMR 11

Figure S14. Homonuclear decoupled ^{1}H NMR 12

Figure S15. ^{1}H NMR spectra of the obtained PVL 12

Figure S16. ^{1}H NMR spectra of the obtained PCL 13

Figure S17. ^{1}H NMR spectra of the obtained PLA 13

4. GPC curves of various polymer 14

Figure S18. GPC curves of the obtained PVL 14

Figure S19. GPC curves of the obtained PCL 14

Figure S20. GPC curves of the obtained PLA at room temperature 14

Figure S21. GPC curves of the obtained PLA at low temperature 15

Figure S22. GPC curves of the obtained PVL 15

Figure S23. GPC curves of the obtained PVL 15

5. Experimental data.....15

Table S1. k_{obs} for δ-VL ROP with NHO3 and different TUs (Us) 16

Table S2. ROPs of δ-VL with various ratios of monomer/initiator.....16

Table S3. The results of monomer conversion and molecular weight versus time 17

6. MALDI-TOF MS spectrum 17

Figure S24. MALDI-TOF MS spectrum of the obtained PCL sample.....17

References.....18

1. General Experimental Procedure

Preparation of NHOs

The depicted *N*-Heterocyclic Olefins (NHOs) have been synthesized according to literature-known procedures. NHOs was synthesized by deprotonation of the corresponding precursor salt (Scheme S1) using KHMDS and they were stored in a glove box at -25 °C. For full characterization of NHO1, NHO2, NHO3, NHO4 and NHO5 see the cited literature.[1-5]

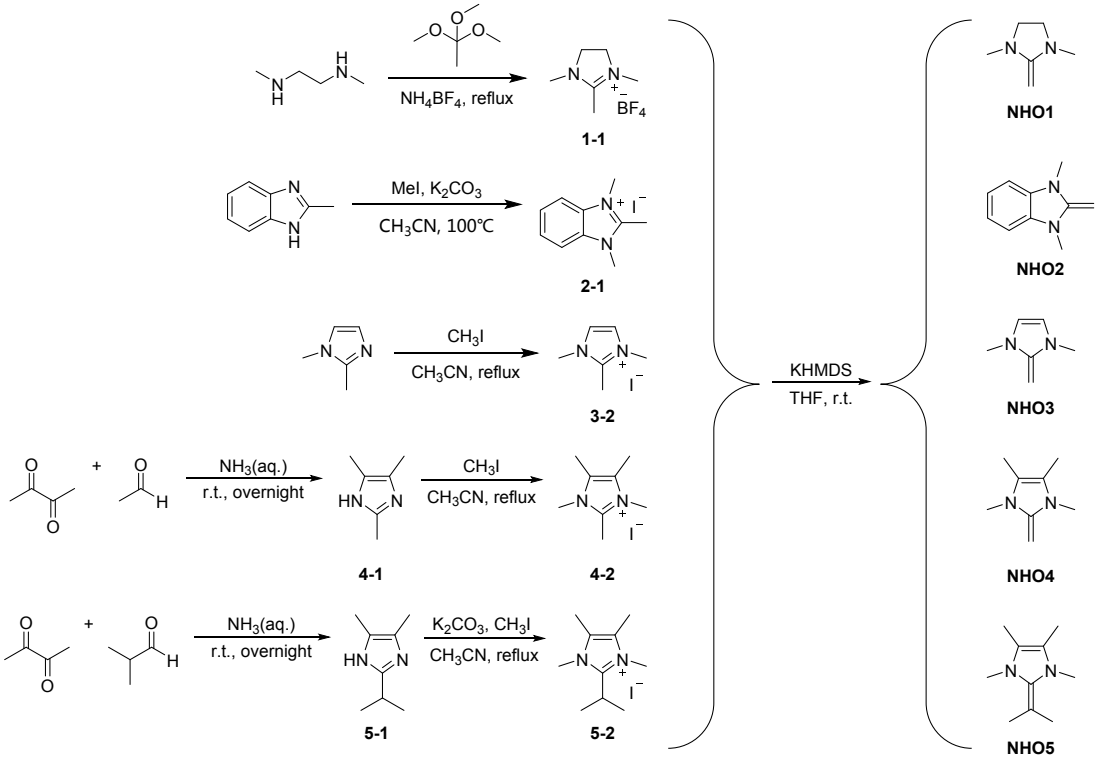

Scheme S1. Synthetic routes for the NHOs employed in this study.

Preparation of TUs/Us

The depicted thioureas (TUs) and ureas (Us) are prepared by mixing the appropriate amine and isothiocyanate in a solution of MeOH (Scheme S2). The solution was stirred in the room temperature for 30 min. Then MeOH is removed under vacuum and the products were purified by washing with hexanes three times. After vacuum

filtration, the filter residue was vacuum drying at 50 ℃ for 24 h. For full characterization of TU1, TU2, TU3, TU4, TU5, TU6, U1, U2 and U8 see the cited literature.[6-10] U3, U4, U5, U6 and U7 were purchased from commercial suppliers and dried under vacuum at 50 ℃ for 24 hours.

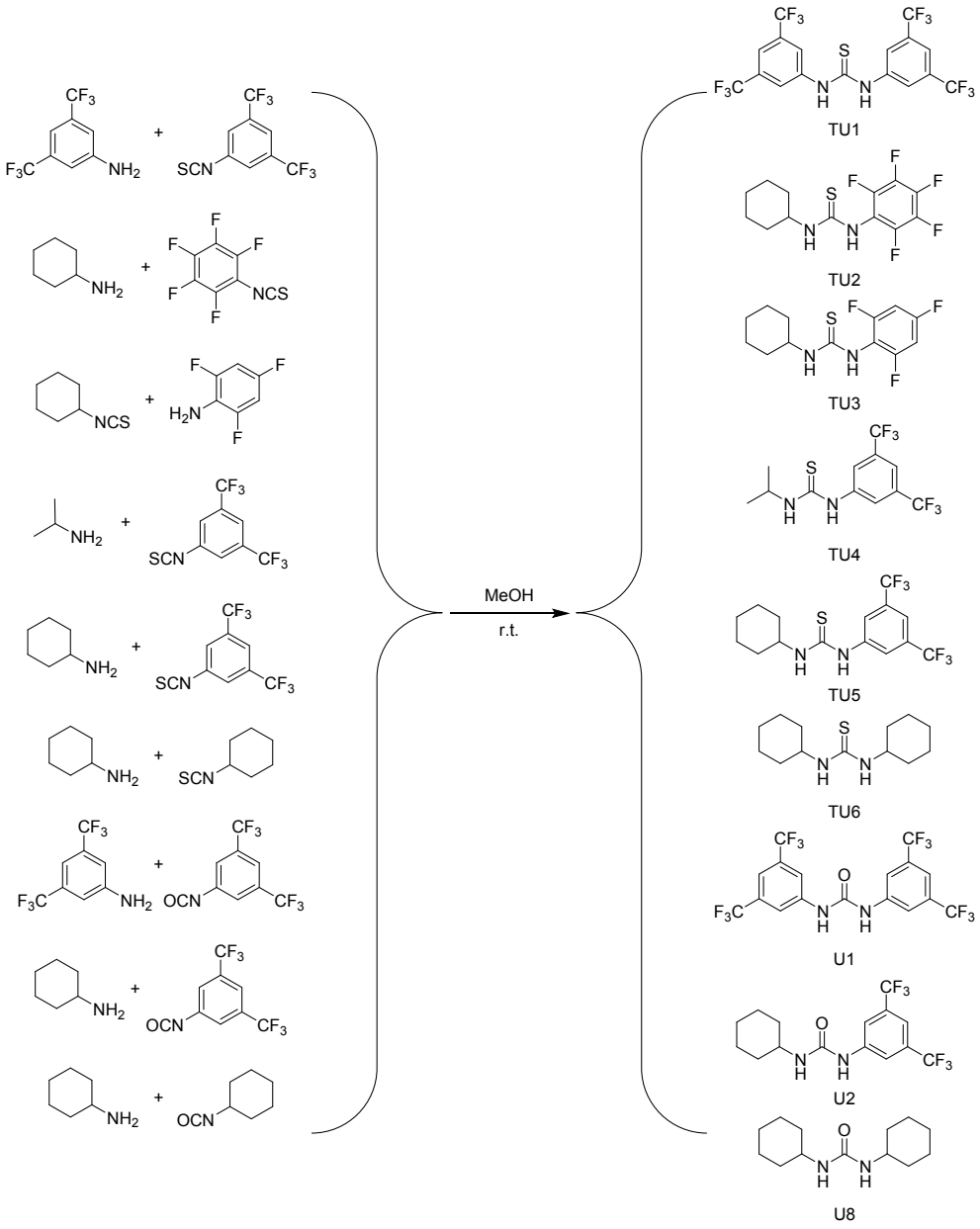

Scheme S2. Synthetic routes for the TUs/Us.

2. pK_a determination of NHOs

When NHOs and BnOH were mixed together, the methylene group of BnOH shifted downfield. The stronger the basicity of NHOs, the greater the chemical shift of the methylene group of BnOH.

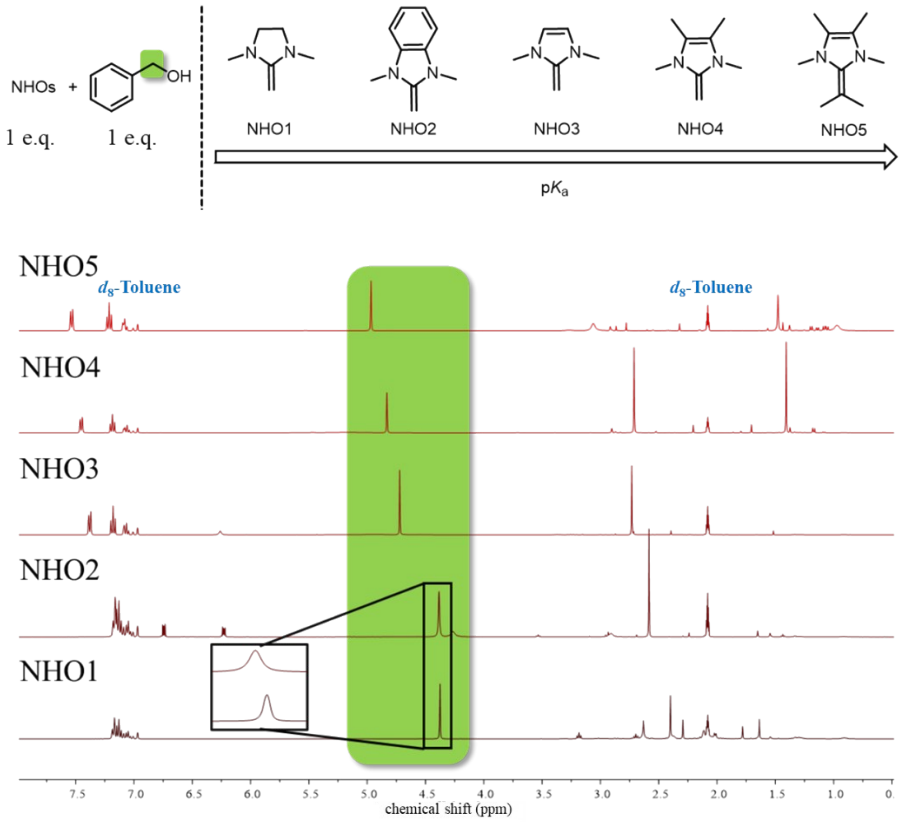

Figure S1. ^{1}H NMR (d_8-Toluene, 400 MHz) of NHOs and BnOH (NHOs:BnOH =1:1).

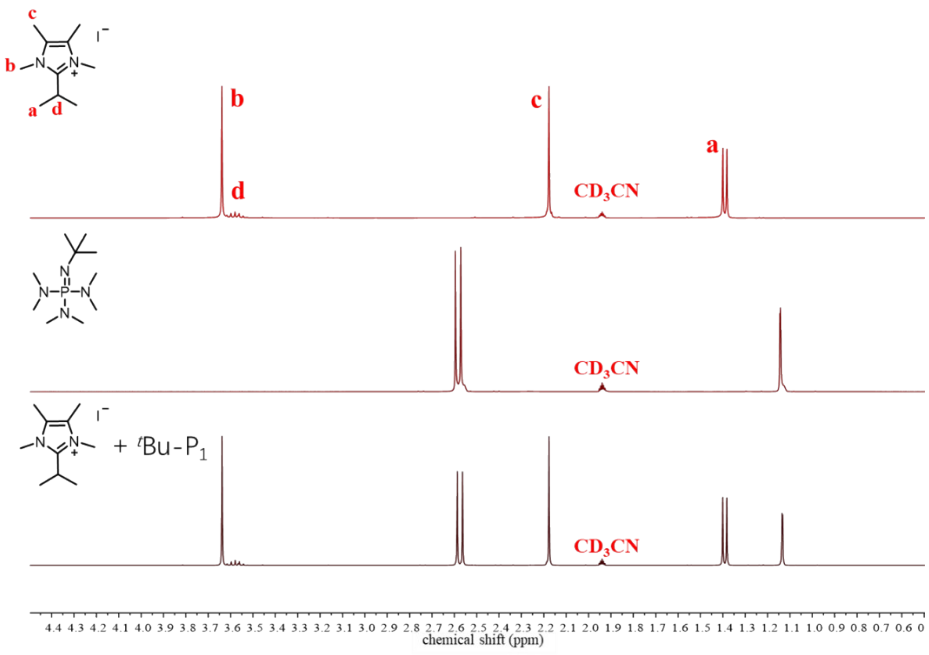

Figure S2. ^{1}H NMR (d_3-MeCN, 400 MHz) of NHO5 precursor salt, ^{t}Bu-P$_1$ and combinations (NHO5 precursor salt: ^{t}Bu-P$_1$ =2:1).

The NMR signal of the "d" methyne group remained unchanged when ^{t}Bu-P$_1$ (pK_a = 26.9) was

used to deprotonate the NHO5 precursor salt, which proves that NHO5 exhibits a higher pK_a than ^{t}Bu-P$_1$ (pK_a[NHO5] > 26.9).

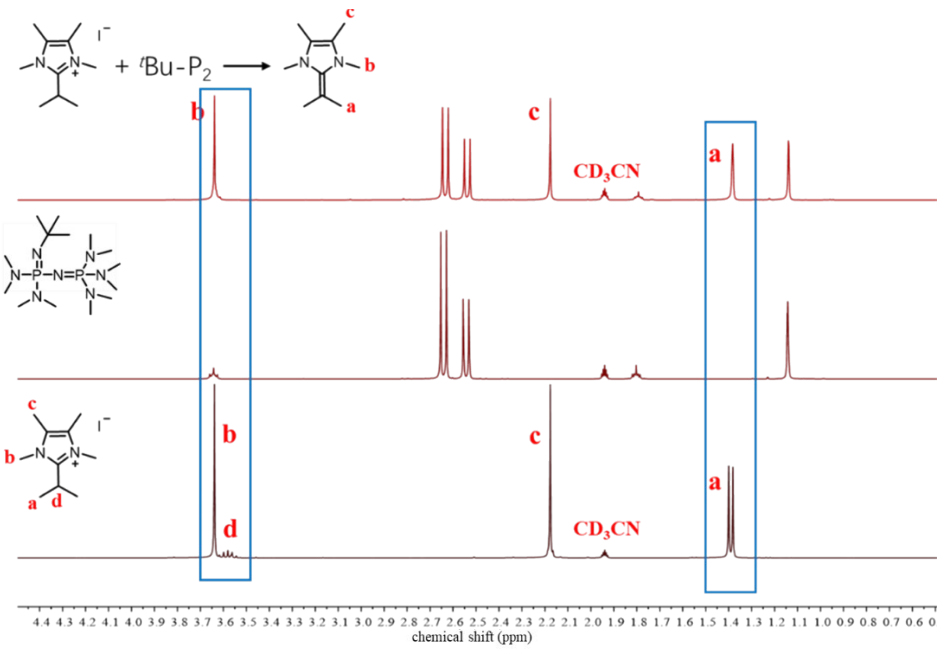

Figure S3. ^{1}H NMR (d_3-MeCN, 400 MHz) of NHO5 precursor salt, ^{t}Bu-P$_2$ and combinations (NHO5 precursor salt: ^{t}Bu-P$_2$ =2:1).

The signal of the "d" methyne group disappeared when the ^{t}Bu-P$_2$ (pK_a = 33.5) base was used for the deprotonation of NHO5 precursor salt, which proves that ^{t}Bu-P$_2$ exhibits a higher pK_a than NHO5 (pK_a[NHO5] < 33.5).

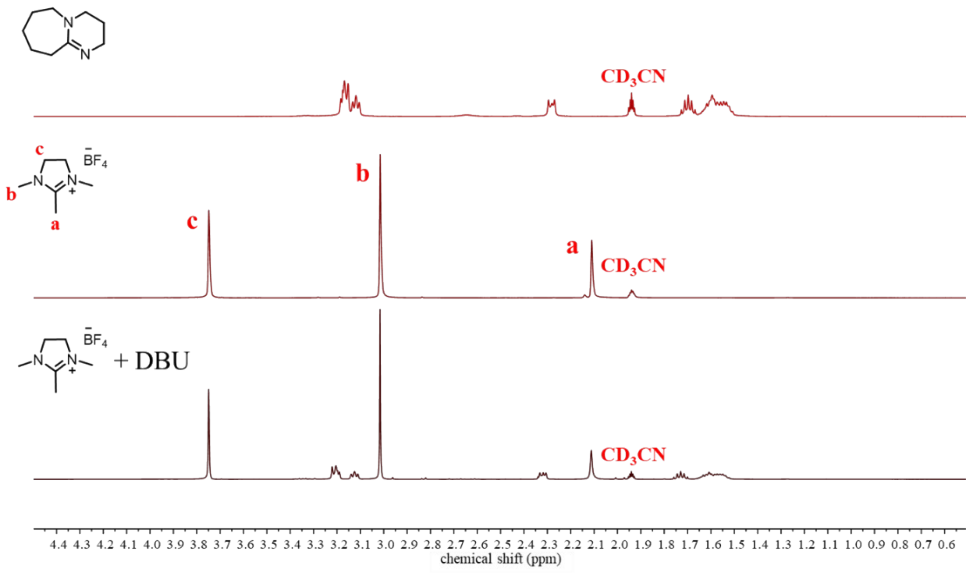

Figure S4. ^{1}H NMR (d_3-MeCN, 400 MHz) of NHO1 precursor salt, DBU and combinations (NHO1 precursor salt: DBU =2:1).

The NMR signal of the “a” methyl group remained unchanged when DBU (pK_a = 24.3) was used to deprotonate the NHO1 precursor salt, which proves that NHO1 exhibits a higher pK_a than DBU (pK_a[NHO1] > 24.3).

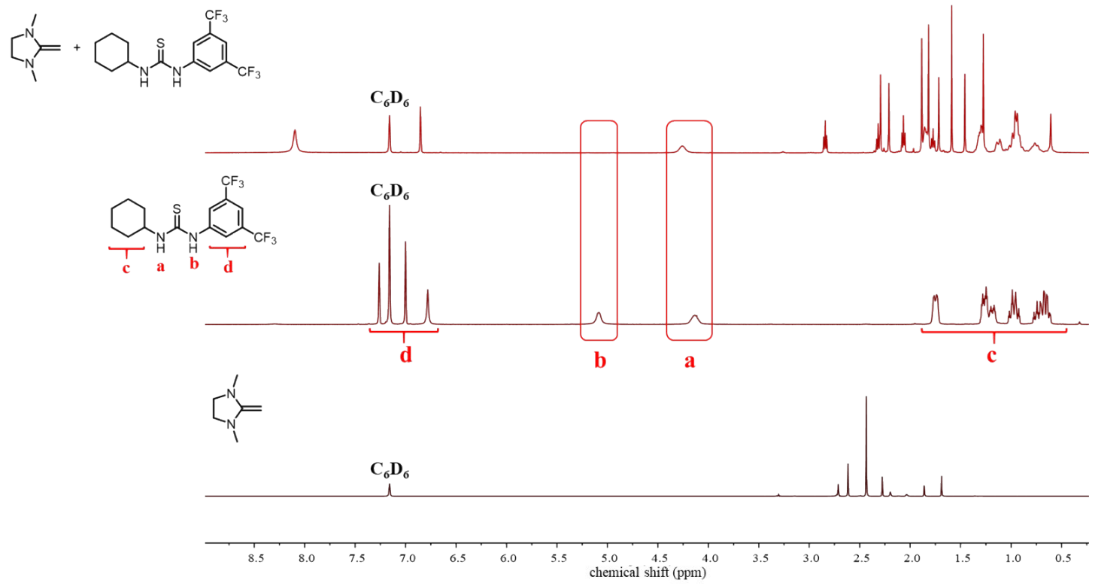

Figure S5. ^{1}H NMR (C_6D_6, 400 MHz) of NHO1, TU5 and combinations (NHO1:TU5=1:1).

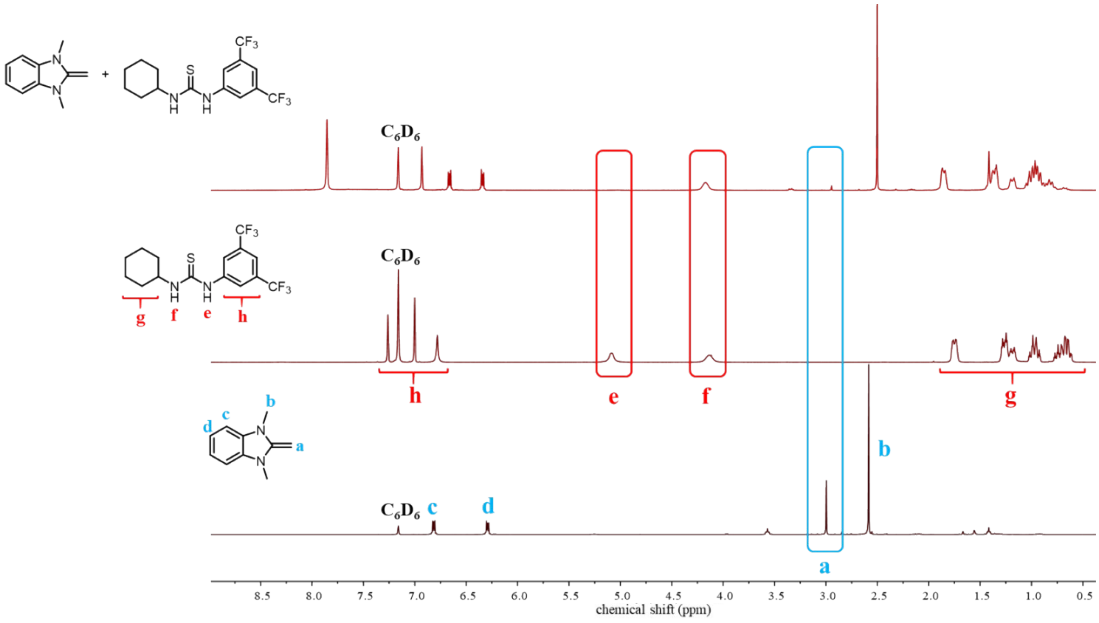

Figure S6. ^{1}H NMR (C_6D_6, 400 MHz) of NHO2, TU5 and combinations (NHO2:TU5=1:1).

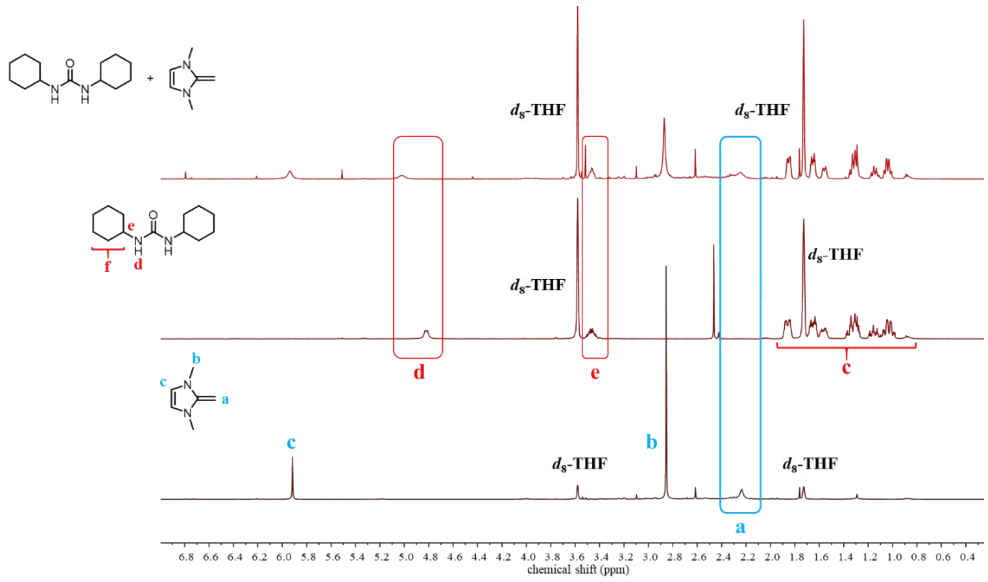

Figure S7. ^{1}H NMR (d_8-THF, 400 MHz) of NHO3, U8 and combinations (NHO3:U8=1:1).

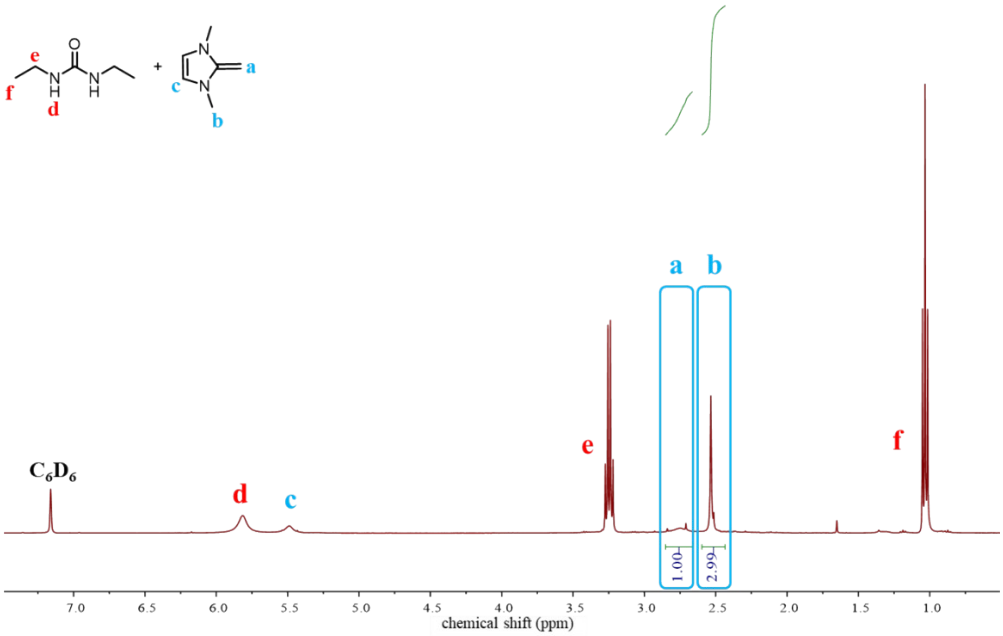

Figure S8. ^{1}H NMR (C_6D_6, 400 MHz) of NHO3 and U6 (NHO3:U6=1:1).

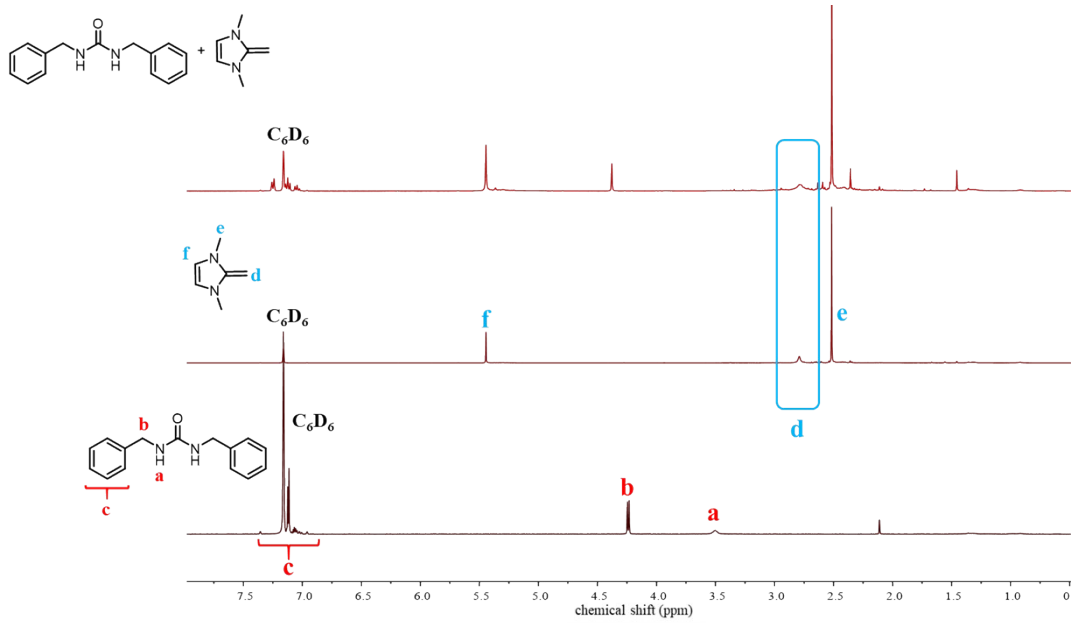

Figure S9. ^{1}H NMR (C_6D_6, 400 MHz) of NHO3, U5 and combinations (NHO3:U5=1:1).

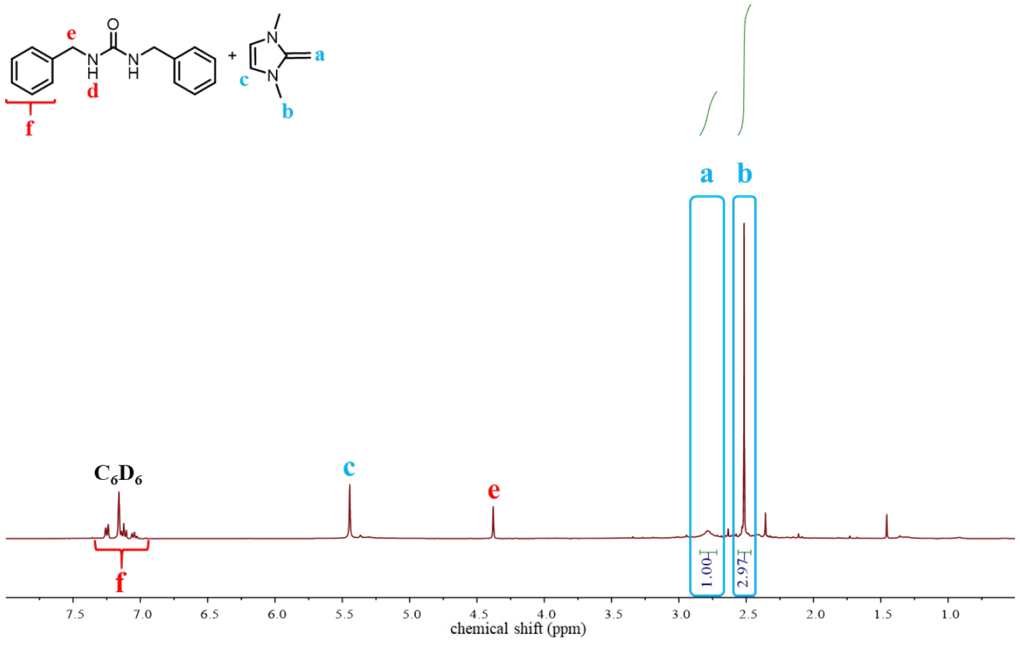

Figure S10. ^{1}H NMR (C_6D_6, 400 MHz) of NHO3 and U5 (NHO3:U5=1:1).

3. ^{1}H NMR Spectra

For homonuclear decoupled ^{1}H NMR analysis, acquisition time was measured and fixed to 2.04 s. Samples were obtained in $CDCl_3$ solutions with the decoupling pulse

based on the methyl region (δ = 1.5 ppm). In case of the good separation of methine region (δ = 5.00-5.20 ppm), both Bernouillan statistics (chain-end control mechanism, CEC) and non-Bernouillan statistics (enantiomorphic site control mechanism, ESC) were used to calculate P_m values.[11]

	Probability of ESC (non-Bernouillan)	Probability of CEC (Bernouillan)
[*mmm*]	$[P_m^2+(1-P_m)^2+P_m^3+(1-P_m)^3]/2$	$P_m^2+0.5\ P_mP_r$
[*rmm*]	$[P_m^2(1-P_m) + P_m(1-P_m)^2]/2$	$0.5\ P_mP_r$
[*mmr*]	$[P_m^2(1-P_m) + P_m(1-P_m)^2]/2$	$0.5\ P_mP_r$
[*rmr*]	$[P_m^2(1-P_m) + P_m(1-P_m)^2]/2$	$0.5\ P_r^2$
[*mrm*]	$[P_m(1-P_m)]$	$0.5\ (P_m^2+P_mP_r)$

P_r has meaning of racemic enchainment, and $P_m+P_r=1$.

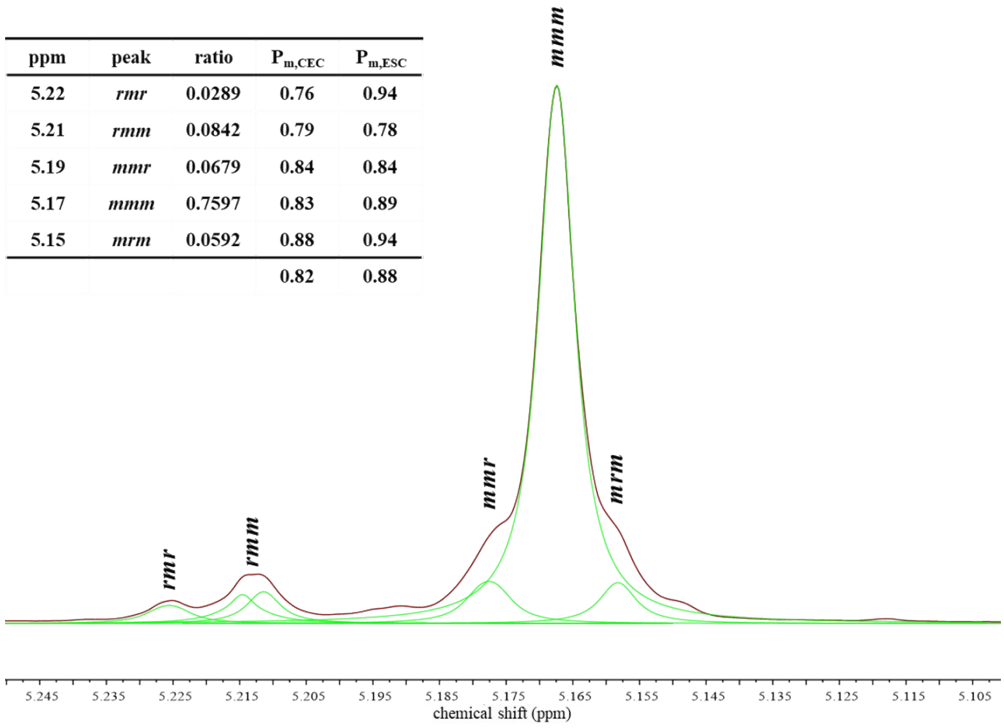

Figure S11. Homonuclear decoupled ^{1}H NMR (Table 4, entry 1).

ppm	peak	ratio	$P_{m,CEC}$	$P_{m,ESC}$
5.22	*rmr*	0.0159	0.83	0.97
5.21	*rmm*	0.0691	0.84	0.83
5.19	*mmr*	0.0090	0.99	0.98
5.17	*mmm*	0.8989	0.93	0.96
5.15	*mrm*	0.0071	0.99	0.99
			0.92	0.95

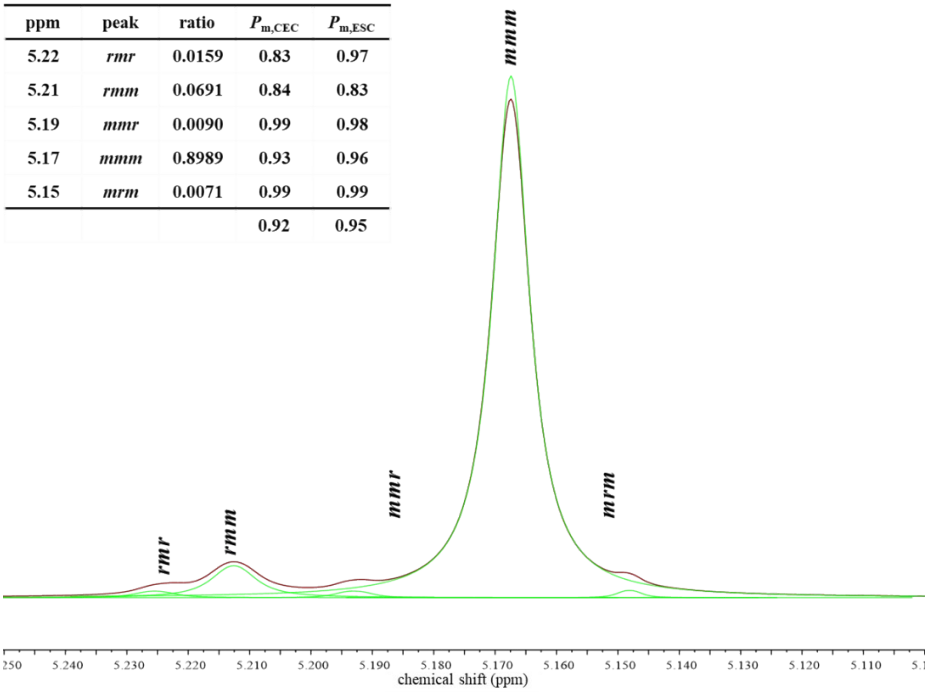

Figure S12. Homonuclear decoupled ^{1}H NMR (Table 4, entry 3).

ppm	peak	ratio	$P_{m,CEC}$	$P_{m,ESC}$
5.22	*rmr*	0.0267	0.77	0.94
5.21	*rmm*	0.0682	0.84	0.84
5.19	*mmr*	0.0065	0.99	0.99
5.17	*mmm*	0.8924	0.93	0.96
5.15	*mrm*	0.0062	0.99	0.99
			0.90	0.94

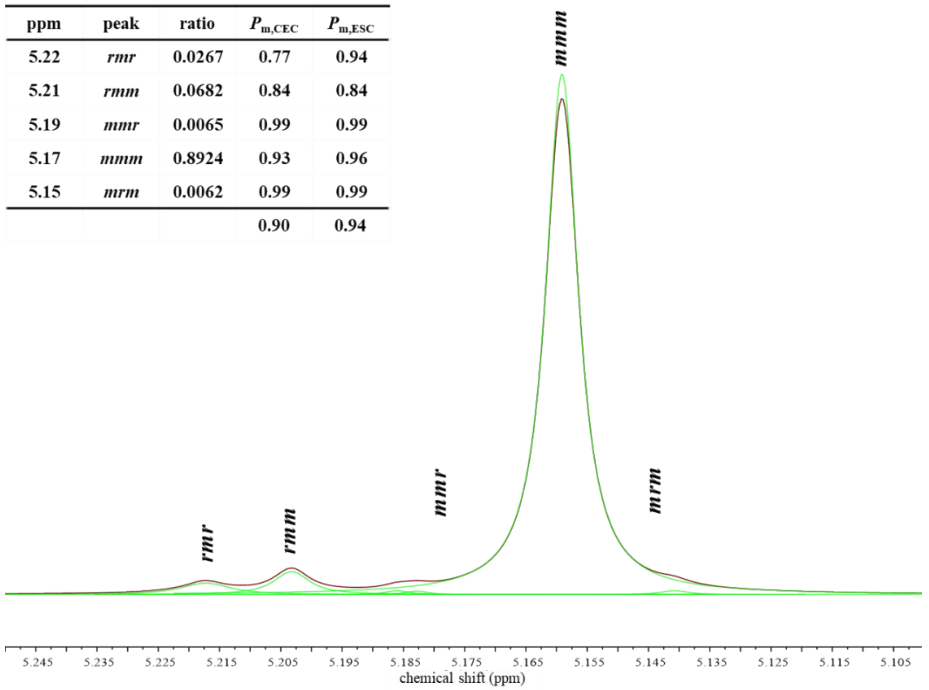

Figure S13. Homonuclear decoupled ^{1}H NMR (Table 4, entry 4).

ppm	peak	ratio	$P_{m,CEC}$	$P_{m,ESC}$
5.22	*rmr*	0.0166	0.82	0.97
5.21	*rmm*	0.0395	0.91	0.91
5.19	*mmr*	0.0479	0.89	0.89
5.17	*mmm*	0.8572	0.9	0.94
5.15	*mrm*	0.0387	0.93	0.96
			0.89	0.93

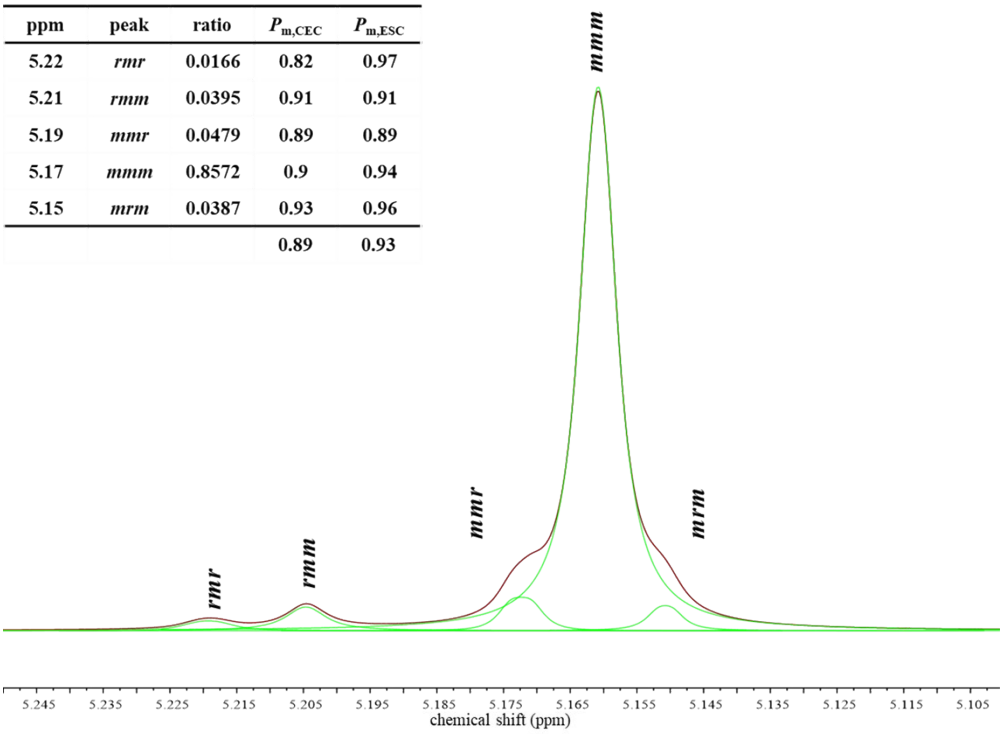

Figure S14. Homonuclear decoupled ^{1}H NMR (Table 4, entry 6).

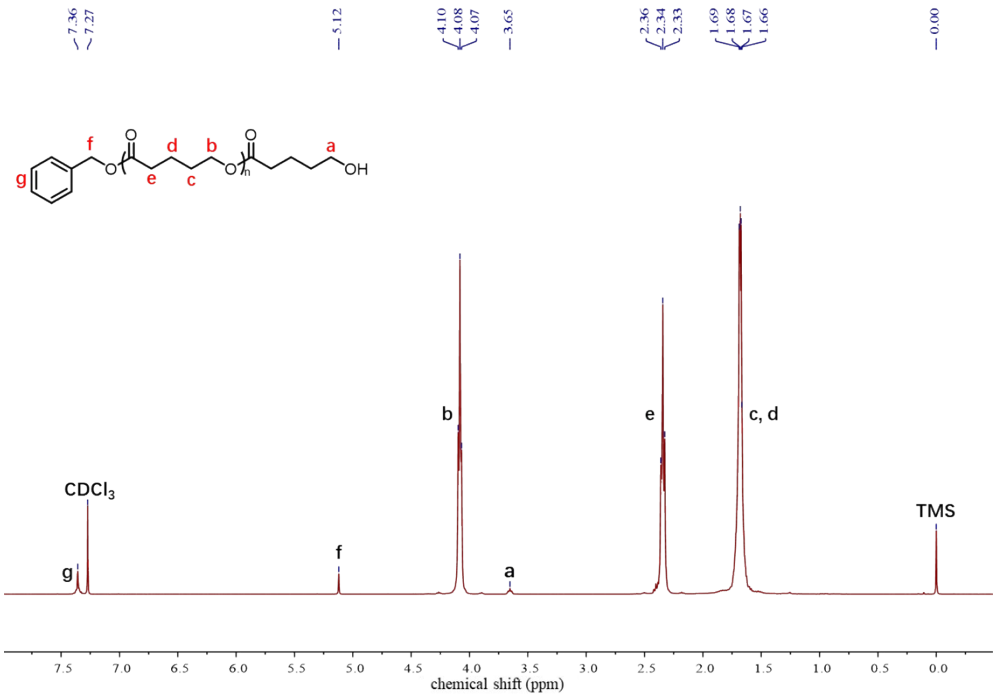

Figure S15. ^{1}H NMR ($CDCl_3$, 400 MHz) spectra of the obtained PVL.

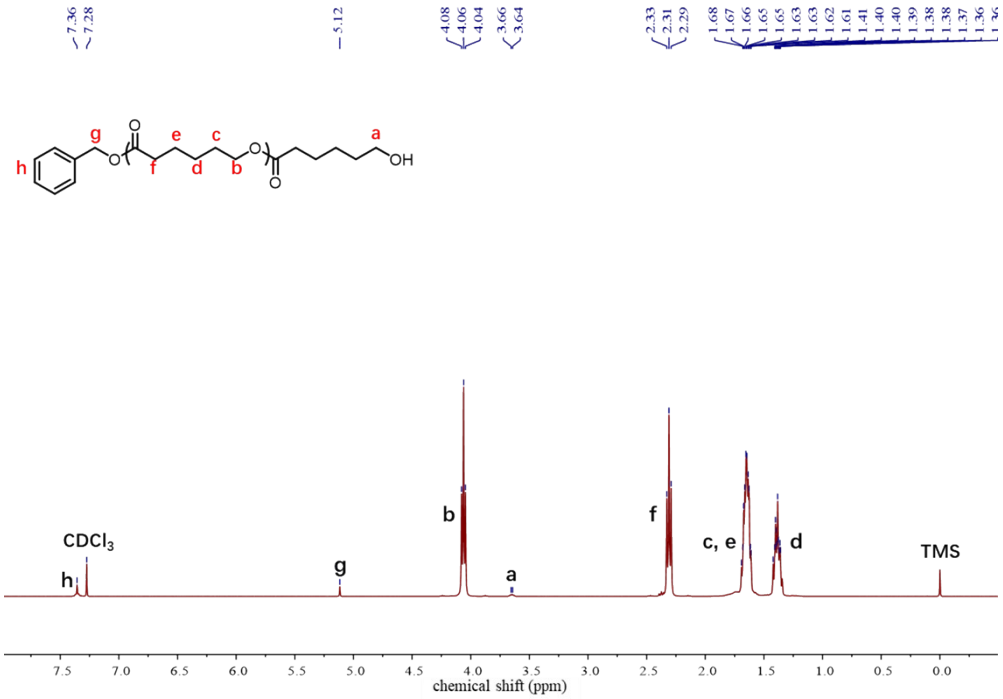

Figure S16. ^{1}H NMR ($CDCl_3$, 400 MHz) spectra of the obtained PCL.

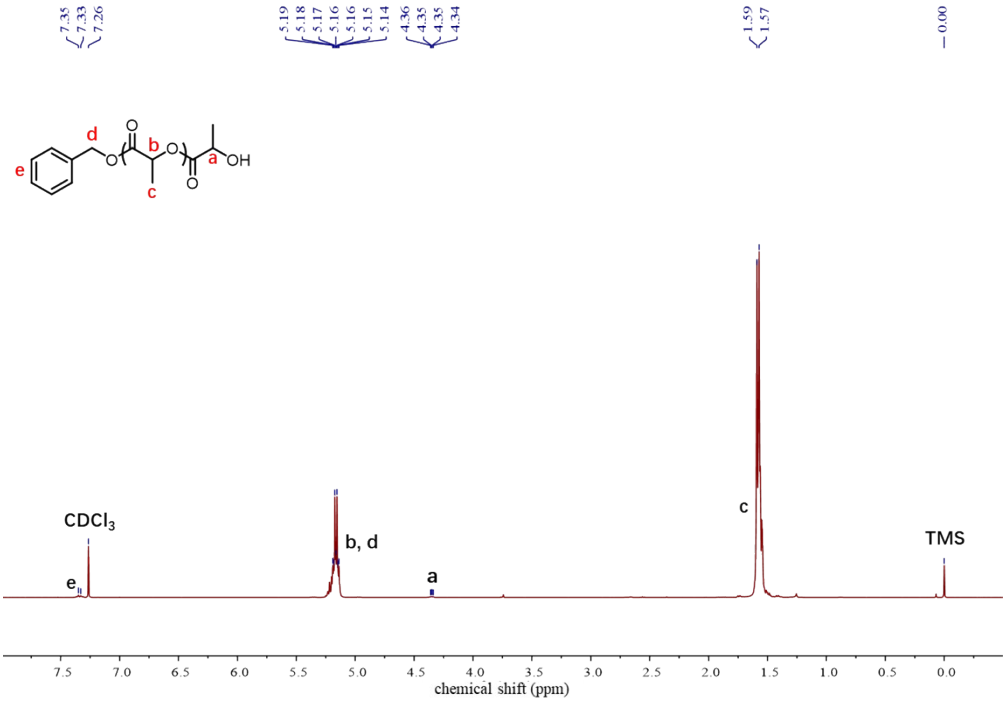

Figure S17. ^{1}H NMR ($CDCl_3$, 400 MHz) spectra of the obtained PLA.

4. GPC curves of various polymer

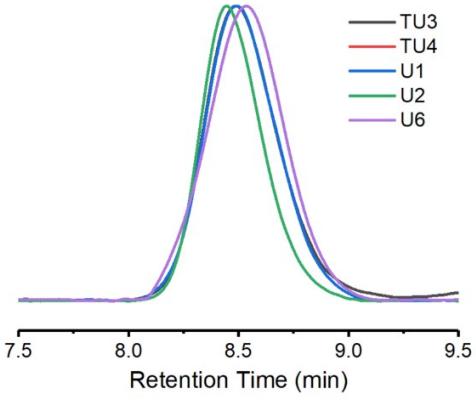

Figure S18. GPC curves of the obtained PVL (Table 1).

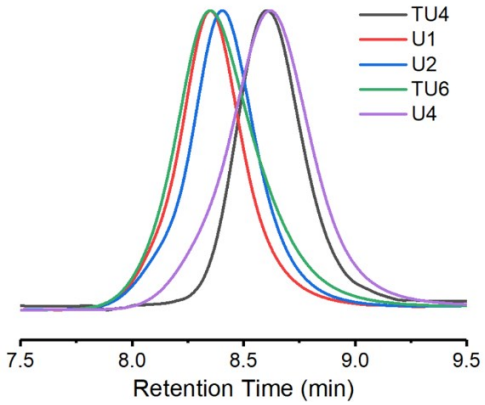

Figure S19. GPC curves of the obtained PCL (Table 2).

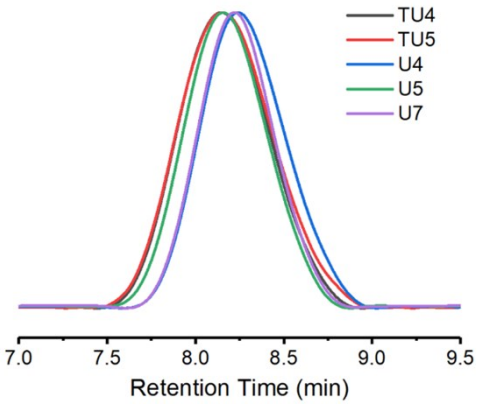

Figure S20. GPC curves of the obtained PLA at room temperature (Table 3).

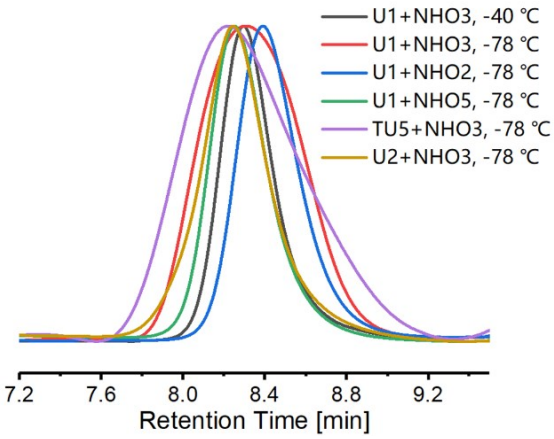

Figure S21. GPC curves of the obtained PLA at low temperature (Table 4).

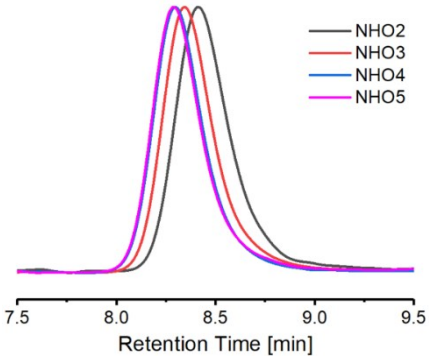

Figure S22. GPC curves of the obtained PVL (Table 5, entries 2-5).

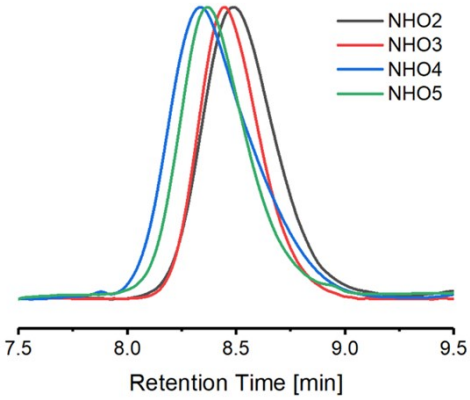

Figure S23. GPC curves of the obtained PVL (Table 5, entries 7-10).

5. Experimental data

Table S1. k_{obs} for δ-VL ROP with NHO3 and different TUs (Us) [a]

TUs/Us	k_{obs} (min^{-1})
TU1	$7.1*10^{-6} \pm 2.1*10^{-8}$
TU2	$7.2*10^{-6} \pm 3.2*10^{-8}$
TU3	$0.00072 \pm 2.4*10^{-5}$
TU4	$0.0016 \pm 6.4*10^{-5}$
TU5	$0.0034 \pm 9.5*10^{-5}$
U1	0.148 ± 0.0031
U2	0.064 ± 0.0018
U3	0.138 ± 0.0013
TU6	0.322 ± 0.013
U4	0.537 ± 0.019
U5	$0.0055 \pm 2.3*10^{-4}$
U6	$0.0014 \pm 6.1*10^{-5}$
U7	$0.0013 \pm 6.5*10^{-5}$
U8	$0.00082 \pm 3.3*10^{-5}$

[a]Reaction conditions: $[NHO3]_0$:$[TU/U]_0$:$[BnOH]_0$:$[VL]_0$ = 1:2:2:800 in toluene at room temperature, $[VL]_0$ = 3.4 mol/L.

Table S2. ROPs of δ-VL with various ratios of monomer/initiator [a]

Entry	NHO3/U1/BnOH/δ-VL	Time	Conv. [b]	$M_{n,cal}$ (g/mol)	$M_{n,\,exp}$ (g/mol) [c]	$Đ$ [c]
1	1/2/2/100	30 s	95 %	4800	5400	1.14
2	1/2/2/200	5 min	98 %	9800	12200	1.15
3	1/2/2/400	10 min	94 %	18800	19500	1.16
4	1/2/2/800	30 min	96 %	38400	34300	1.22

[a] Polymerization conditions: room temperature, toluene as solvent, the reactions were carried in sealed tube. [b] Determined by ^{1}H NMR in $CDCl_3$ using integrals of the characteristic signals. [c] Number-average molar mass (M_n) and dispersity values were determined by GPC in THF at 25 °C using polystyrene standards for calibration, and corrected using the factor 0.57 for PVL.

Table S3. The results of monomer conversion and molecular weight versus time [a]

Time	Conv. [b]	$M_{n,cal}$ (g/mol)	$M_{n,exp}$ (g/mol) [c]	$Đ$ [c]
30 min	8 %	4600	4200	1.12
2 h	26 %	14800	13300	1.10
4 h	51 %	29100	22300	1.15
6 h	68 %	38800	31000	1.18
8 h	80 %	45700	38100	1.21
10 h	98 %	55900	46100	1.46

[a] Unless otherwise specified, reaction conditions are $[NHO3]_0$:$[U1]_0$:$[BnOH]_0$:$[ε\text{-}CL]_0$ = 1:2:2:1000 in toluene at room temperature. [b] Determined by ^1H NMR in $CDCl_3$ using integrals of the characteristic signals. [c] Number-average molar mass (M_n) and dispersity values were determined by GPC in THF at 25 °C using polystyrene standards for calibration, and corrected using the factor 0.56 for PCL.

6. MALDI-TOF MS spectrum

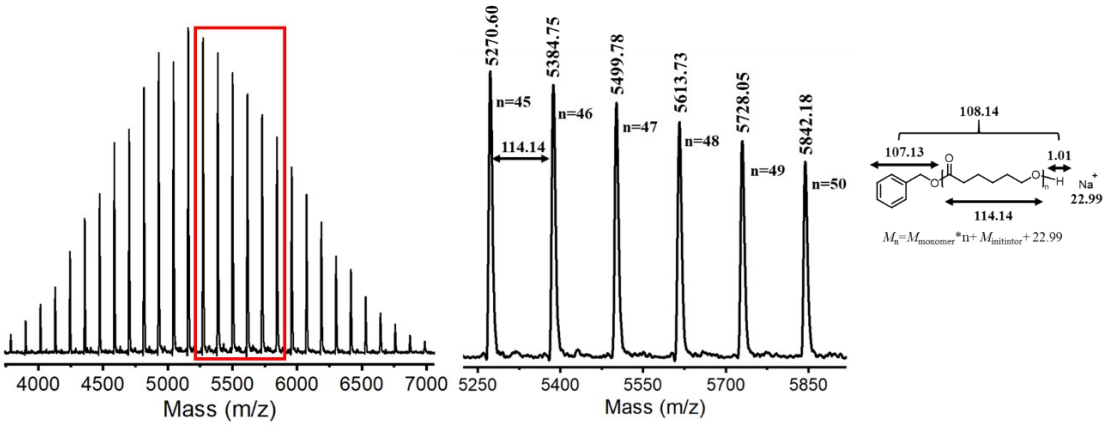

Figure S24. MALDI-TOF MS spectrum of the obtained PCL sample (NHO3/U1/BnOH/ε-CL= 1:2:2:200).

References

1. W.-C. Chen, J.-S. Shen, T. Jurca, C.-J. Peng, Y.-H. Lin, Y.-P. Wang, W.-C. Shih, G. P. A. Yap and T.-G. Ong, *Angew. Chem., Int. Ed.*, 2015, **54**, 15207-15212.
2. S. Naumann, A. W. Thomas and A. P. Dove, *Angew. Chem., Int. Ed.*, 2015, **54**, 9550-9554.
3. V. B. Saptal and B. M. Bhanage, *ChemSusChem*, 2016, **9**, 1980-1985.
4. P. Walther, W. Frey and S. Naumann, *Polym. Chem.*, 2018, **9**, 3674-3683.
5. S. Kronig, P. G. Jones and M. Tamm, *Eur. J. Inorg. Chem.*, 2013, **13**, 2301-2314.
6. V. Štrukil, M. D. Igrc, M. Eckert-Maksić and T. Friščić, *Chem. Eur. J.*, 2012, **18**, 8464-8473.
7. C. B. Tripathi and S. Mukherjee, *Org. Lett.*, 2014, **16**, 3368-3371.
8. J. Sun, and D. Kuckling, *Polym. Chem.*, 2016, **7**, 1642-1649.
9. Z.-L. Jiang; J.-P. Zhao and G.-Z. Zhang, *Chinese J. Polym. Sci.*, 2019, **37**, 1205-1214.
10. L. Zhou, G. Xu, Q. Mahmood, C. Lv, X. Wang, X. Sun, K. Guo and Q. Wang, *Polym. Chem.*, 2019, **10**, 1832-1838.
11. B. Orhan, M. J.-L. Tschan, A.-L. Wirotius, A. P. Dove, O. Coulembier and D. Taton, *ACS Macro. Lett.*, 2018, **7**, 1413-1419.